R.W. de Boer[1])

Magnetization transfer contrast

Part 1: MR physics

One of the principle advantages of Magnetic Resonance Imaging (MRI) over other diagnostic imaging modalities is the intrinsically large bandwidth of soft tissue contrast. Traditionally, clinical imaging exploits the contrast due to differences in spin density (ρ), spin-lattice relaxation (T_1), and spin-spin relaxation (T_2) between normal tissues and pathology.

However, other contrast mechanisms such as susceptibility, magnetization transfer, chemical shift, diffusion, perfusion, flow, and endogenous and exogenous agents can be used to create specific and subtle changes in contrast. One of these mechanisms, magnetization transfer, has been actively researched during the last couple of years, following Wolff and Balaban's publication of their first results[4].

Magnetization Transfer Contrast (MTC) in magnetic resonance imaging is the result of selectively observing the interaction of bulk water protons with the protons contained in macromolecules of tissue.

Magnetization Transfer (MT) is based on well-defined biophysical and biochemical properties. Since different tissues have different macromolecular compositions, the degree of interaction, or Magnetization Transfer (MT), can differ widely, generating very high tissue contrast.

MTC is obtained by combining saturation transfer techniques with standard MRI procedures. The basic use of the saturation transfer technique in MR spectroscopy was already described in 1963 by Forsén and Hoffman[1], who used it to calculate the exchange rate of specific chemical reactions. In the 1970's Edzes and Samulski[2, 3] proposed that cross-relaxation between ^1H pools was a dominant relaxation mechanism in biological systems such as collagen and muscle. However, it was not until 1989 that Wolf and Balaban[4] became the first to apply these principles to in vivo measurements. They calculated the pseudo-first-order rate constant for the transfer of magnetization in kidney and skeletal muscle, and showed images where the contrast was a function of magnetization transfer. In their first publication[4] they predicted that: 'Since the image contrast generated using this method is specific to the exchange between mobile and restricted protons, this technique may prove valuable in diagnosis or characterization of cancer, oedema, or other pathologies where the specific relaxation mechanism may be useful in determining the nature of the disease'.

More experiments[5] were performed on a 4.7 T system and substantiated the original findings. In 1991, the first magnetization transfer images of a cat head at 1.5 T were produced by Wolf, Eng, and Balaban[6]. Their conclusion that 'this technique for increasing tissue contrast has the potential to be applied to imaging human beings at clinically relevant magnetic fields' can be considered as the beginning of a steady stream of scientific papers on MR physics and clinical applications of magnetization transfer contrast. A number of different review papers have recently been published on the various aspects of MTC[7, 10]. In this review, simplified schematic drawings are used to explain the physical properties of MTC for those readers who are less specialized in mathematics and physics.

MR physics of magnetization transfer: relaxation mechanisms

In biological systems, hydrogen nuclei or protons (^1H) can be described as existing in two pools. The so-called 'free pool' consists of relatively mobile protons (correlation times $\approx 3 \cdot 10^{-12}$ s) in free bulk water and some lipid-containing tissues. This pool has a narrow spectral line (10-100 Hz) and a relatively long T_2 (> 10-100 ms), and is labelled in mathematical descriptions as the A pool. With standard MRI this pool provides the bulk of the signal.

The second pool or 'bound pool' consists of restricted protons bound in proteins, other large

[1]) Philips Medical Systems, Best, the Netherlands.

macromolecules, and cellular membranes. This pool has a very broad spectral line (10-50 kHz) and subsequently a very short T_2 (< 0.1 ms), and is labelled in mathematical descriptions as the B pool. With conventional MRI this pool is not 'MR visible', because its signals are not directly detectable due to the very short T_2.

Note that both pools have approximately the same central resonance frequency (Fig. 1) and that the only difference is the larger spread in resonance frequencies of the restricted protons (correlation times ≈ 10^{-8} s).

Under normal MR conditions magnetization is exchanged from the 'free pool' to the 'bound pool' and vice versa, resulting in an equilibrium situation characteristic for that type of tissue. One should realize that if the magnetization in either pool is perturbed (e.g. by the RF excitation pulses in standard MRI), changes occur in both pools. The normally observed spin-lattice relaxation of the 'free pool' is, in fact, a complex function of the recovery of both pools to the equilibrium state (relaxation coupling).

A special situation occurs when the 'bound pool' is *selectively* saturated. This will result in no net magnetization of the 'bound pool' and thus a difference in magnetization between the pools is created. Due to cross relaxation processes, magnetization is transferred from the 'free pool' to the 'bound pool'.

In order to obtain a first order impression of the magnetization transfer phenomenon, a simplified biological tissue with only one imaging voxel is shown in Figure 2. This hypothetical tissue has a 'free pool' of four water molecules with four proton spins, and a 'bound pool' of one macromolecule with three proton spins. In Figures 2-6 the arrow up denotes one unit of measurable MR signal for the 'free pool', and the arrow down indicates zero measurable MR signal. The 'free pool' and 'bound pool' can transfer magnetization to and from each other and are in equilibrium. In the present constellation the signal to noise ratio (S/N) = 4 arbitrary units (AU). Note that the three spins of the 'bound pool' do not contribute to the S/N of this tissue.

The second step of the MTC experiment is to *selectively* saturate the bound protons (Fig. 3). Note that the four spins of the 'free pool' are not (yet) affected. As an example for this specific tissue, the next step in the MT process is that two spins exchange magnetization. The result of this cross relaxation is that the S/N is decreased to 2 AU (Fig. 3). Note that the two spins of the 'bound pool' are 'MR invisible' and therefore do not contribute to the S/N of the tissue. If the 'bound pool' is held in saturation, a new equilibrium situation has been created where the tissue has less available longitudinal magnetization. Note that the apparent longitudinal relaxation time T_{1sat} has been shortened compared to the normal T_1: after excitation it now takes less time to relax back to the new (smaller) equilibrium magnetization (Fig. 4). How this mechanism can actually be used to improve contrast in MRI is shown in Figure 5. We now have two hypothetical tissues. The outside tissue has only four free water molecules with four spins, whereas the inner tissue has both a 'free pool' and a 'bound pool' with also a total of four 'MR visible' spins. Both tissues have a S/N = 4 AU, and therefore there is no contrast.

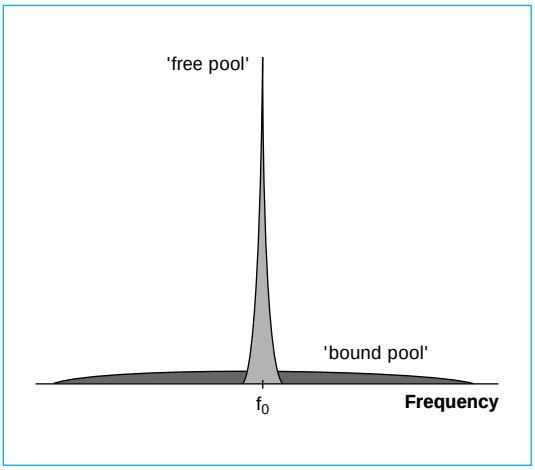

1

Fig. 1. The spectral lines of the 'free pool' and the 'bound pool' are both centred at the same Larmor frequency f_0. The 'free pool' has a narrow line (relatively long T_2); the 'bound pool' has a homogeneous broadened line (T_2 < 0.2 ms).

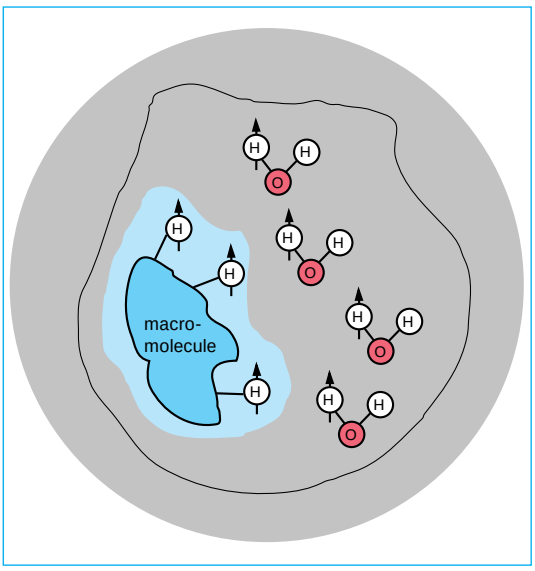

2

Fig. 2. Simplified biological tissue consisting of one imaging voxel. This hypothetical tissue has a 'free pool' of four water molecules with four proton spins, and a 'bound pool' of one macromolecule with three proton spins. An arrow up indicates one unit of measurable MR signal (S/N) for the 'free pool'. An arrow down means no measurable MR signal (S/N = 0).

However, after selective saturation of the 'bound pool' the S/N of the inner tissue is reduced to 2 AU as a result of magnetization transfer. The other tissue is not affected (S/N = 4 AU). Consequently, in the new equilibrium situation, there is a large contrast between the two tissues: namely the Magnetization Transfer Contrast (MTC) (Fig. 5).

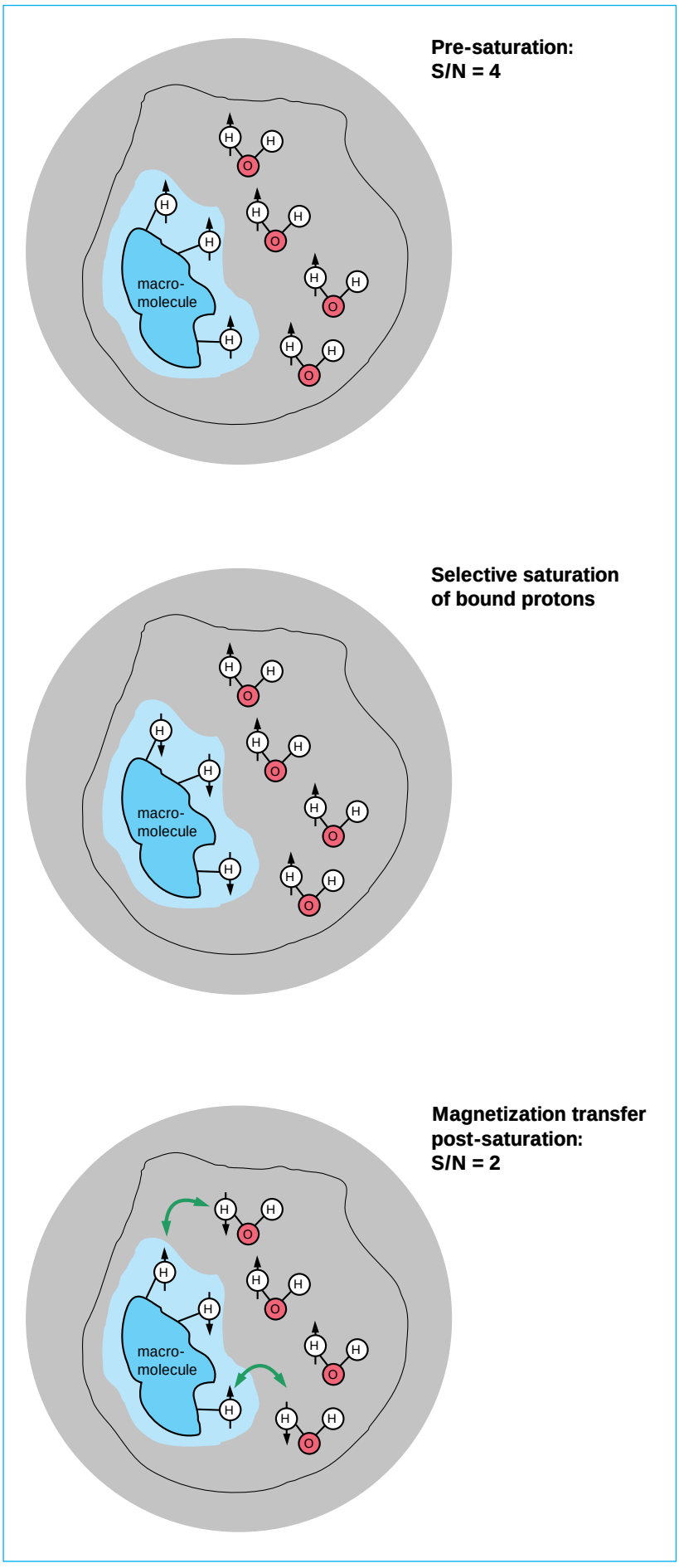

3

Fig. 3. During an MTC experiment the measurable MR signal is decreased. The upper part shows the initial magnetic environment of the hypothetical tissue in Fig. 2, the middle part shows the spins after selective saturation of the 'bound pool', and the bottom image shows the new equilibrium situation with a lower signal of the 'free pool'.

Fig. 4. The apparent longitudinal relaxation time T_{1sat} has been shortened compared with the normal T_1: after excitation it now takes less time to relax back to the equilibrium magnetization M_{Asat}.

Cross relaxation: dipole-dipole interactions

Although the magnetization transfer mechanism is relatively well understood at the tissue

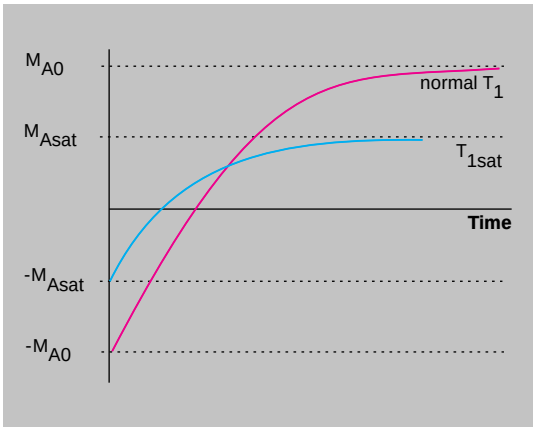

4

level, much less detailed knowledge is available on a cellular and molecular level. Continued advances in modelling of magnetization transfer effects will improve the detailed picture of the mechanism underlying this phenomenon[11, 21]. The most comprehensive models, as summarized by Balaban and Ceckler[7], describe the 'free proton pool' and the macromolecule proton pool ('bound pool'). The 'free pool' is thought to include both mobile bulk water molecules and water molecules bound to the macromolecular surface, the so-called 'hydration water' or 'surface water layer'. These two water fractions exist in a state of rapid chemical equilibrium, such that all the tissue water can be thought of as a single proton pool. According to Eng et al.[5] the surface layer of water communicates with the bulk water by diffusion. The actual transfer of magnetization (see also Figure 6) from the surface layer of water with the macromolecule protons occurs by means of dipole-dipole interactions through space (cross relaxation).

Research on the actual binding sites is ongoing. Eng et al.[5] suggest that lipid bilayers

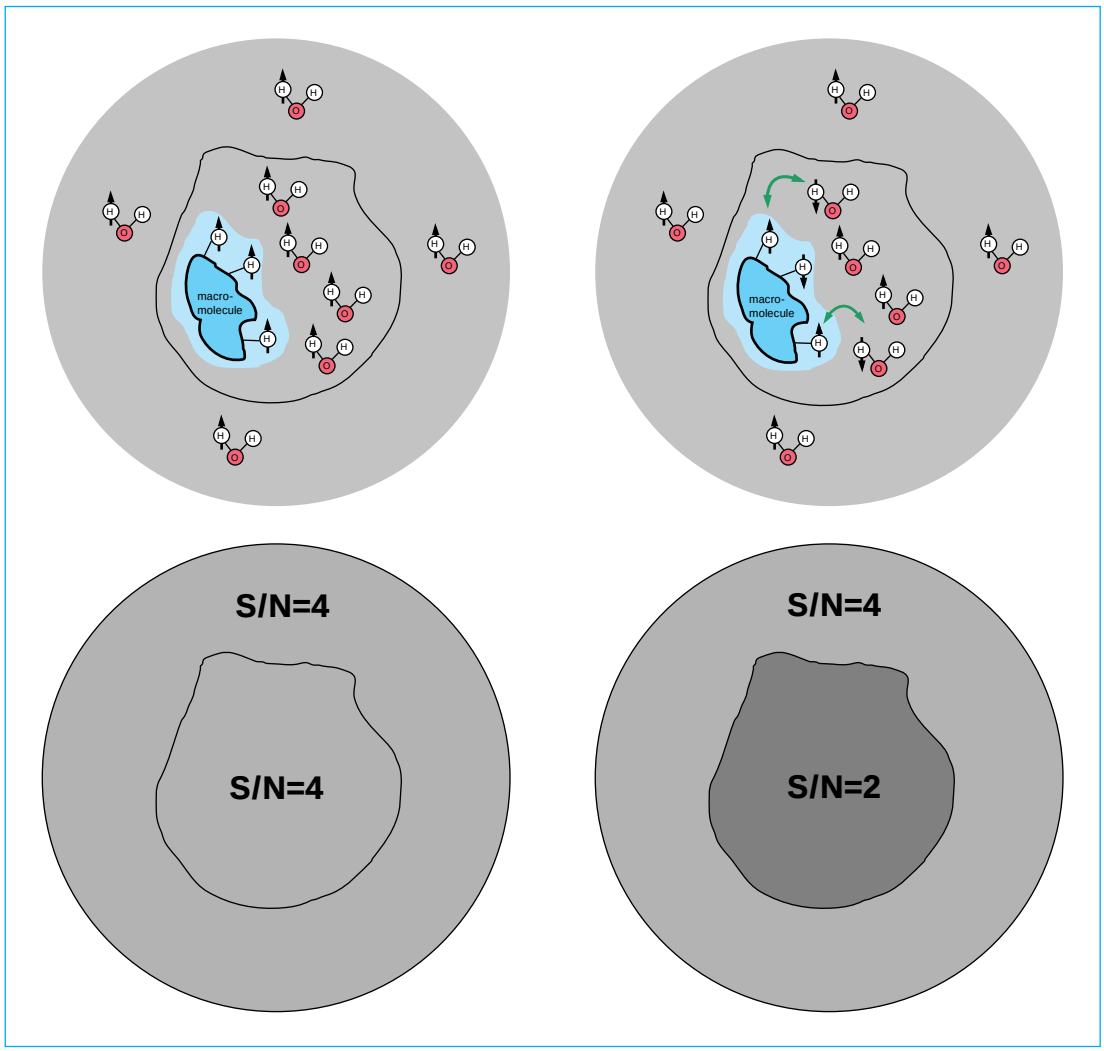

5

Fig. 5. Magnetization transfer can increase contrast between tissues with different biophysical properties. The images on the left represent the pre-MTC situation; those on the right the post-MTC situation. The upper set of drawings show the proton spins in the different tissues. The lower set of images are grey scaled to represent the corresponding signal level.

Fig. 6. Different physical and chemical processes play a role in magnetization transfer: diffusion, chemical exchange, and cross relaxation. For further details, please refer to the main article.

are effective macromolecular structures for magnetization transfer between 'bound' and 'free' protons.

It has also been suggested that chemical exchange between protons in hydration water and macromolecule protons could be the primary mechanism for magnetization transfer. However, experiments with 'broad' ^{2}H spins and water ^{2}H *in vivo*, as well as experiments with the spin ½ isotope tritium, did not reveal magnetization transfer effects. Furthermore, in model lipid systems and other macromolecules, similar magnetization transfer effects have been observed independently of pH values from 5 to 8.

From these studies it is concluded that chemical exchange is not a significant factor in the magnetization transfer process[5].

It is to be expected that ongoing studies will explore the biochemical and biophysical pathways underlying the magnetization transfer mechanism, in order to optimize the specificity of MR tissue characterization with this unique physical phenomenon[9].

6

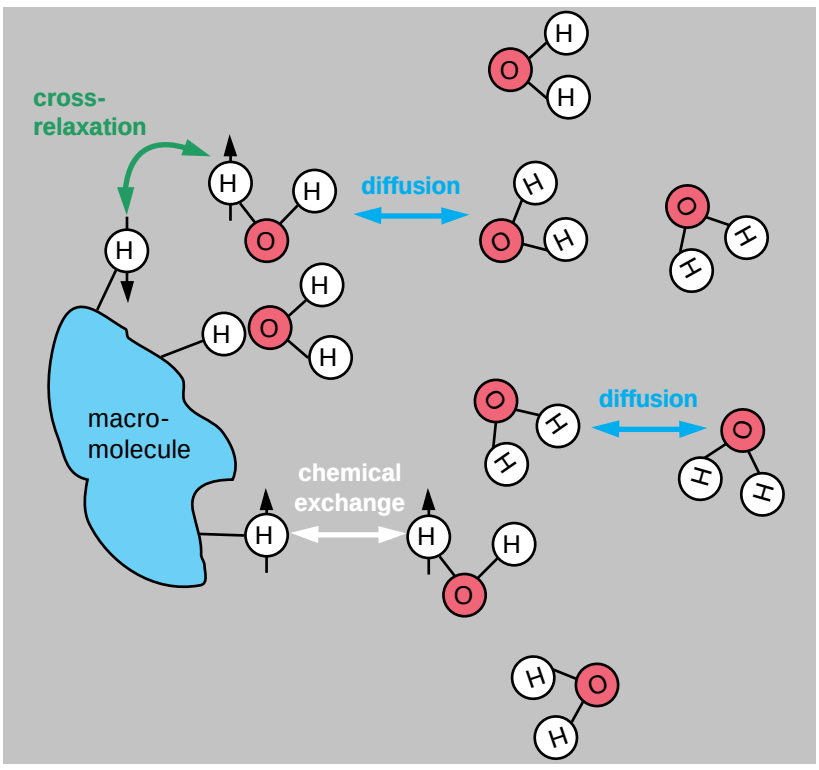

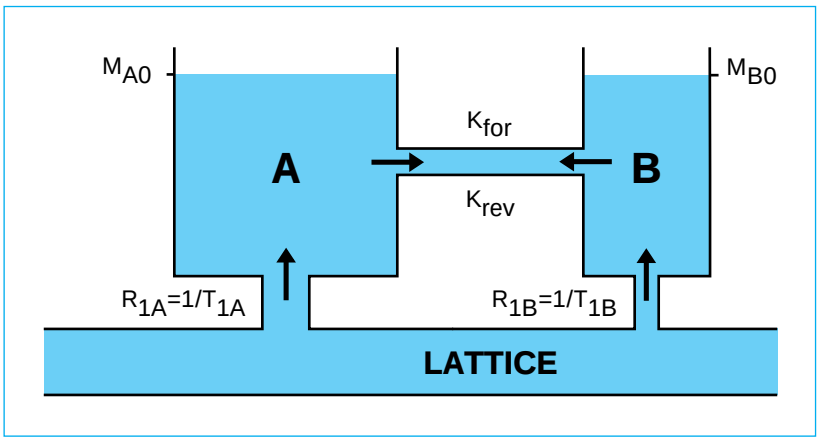

7

Fig. 7. The 'coupled bathtub' model. The A pool is the 'free pool', the B pool is the 'bound pool'. The longitudinal magnetization of the A pool is labelled M_{A0}, and for the B pool M_{B0}. The spin-lattice relaxation rates in the absence of exchange are labelled R_{1A} ($R_{1A} = 1/T_{1A}$) and R_{1B} ($R_{1B} = 1/T_{1B}$). The exchange rates of magnetization transfer between the A and B pool are labelled K_{for} and K_{rev}. The water level in the bathtubs represents the amount of magnetization.

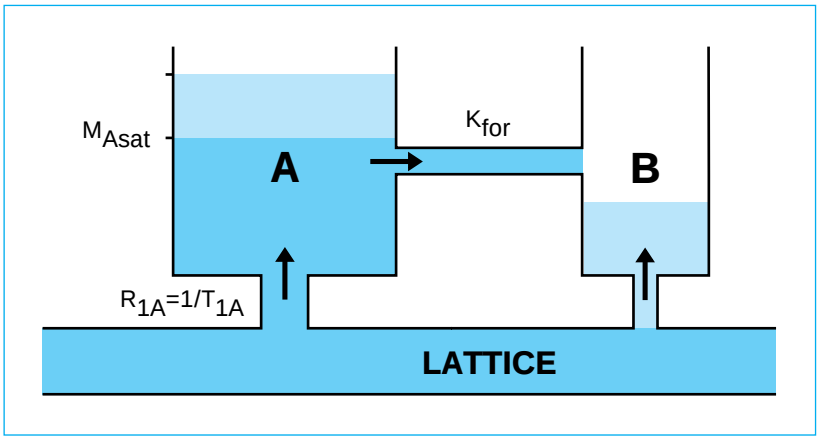

8

Fig. 8. When the B pool is selectively saturated, a new equilibrium is created where the A pool has less available longitudinal magnetization (labelled M_{Asat}). See also Figure 7.

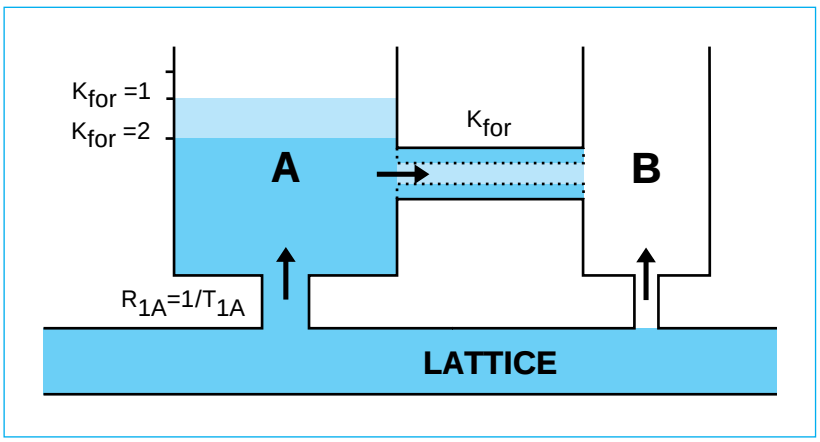

9

Fig. 9. A larger exchange rate K_{for} will result in a lower value for M_{Asat}. The labels K_{for} =1 and K_{for} =2 indicate the magnitude of the longitudinal magnetization M_{Asat} in the two situations. See also Figures 7 and 8.

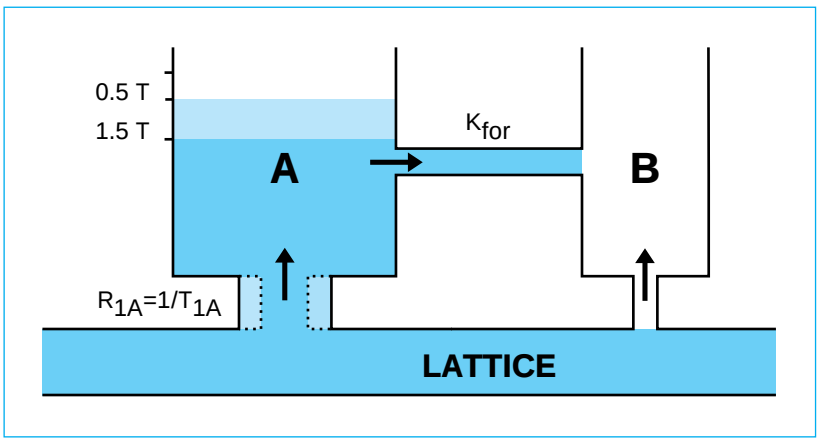

10

Fig. 10. A larger relaxation time T_{1A} will result in a lower value for M_{Asat}. The labels 0.5 T and 1.5 T indicate the magnitude of the longitudinal magnetization M_{Asat} at different field strengths. K_{for} is the same for both situations. See also Figures 7 and 8.

Dynamics of the magnetization transfer mechanism

The dynamics of the magnetization transfer process were already formulated in 1963 by Forsén and Hoffman[1]. A two-pool spin exchange system, shown in Figure 7 by the 'coupled bathtubs' diagram, has been analysed to form a quantitative basis of the previously described mechanisms[22-27, 32]. The longitudinal magnetization of the A pool is labelled M_A, and for the B pool M_B. Under fully relaxed conditions, this is M_{A0} and M_{B0}.

The spin-lattice relaxation rates in the absence of exchange (intrinsic relaxation) are labelled R_{1A} ($R_{1A} = 1/T_{1A}$) and R_{1B} ($R_{1B} = 1/T_{1B}$).

The exchange rates of magnetization transfer between the A and B pools are labelled K_{for} and K_{rev}.

The water level in the bathtubs (Figs 7-10) represents the amount of magnetization.

At equilibrium the transfer of magnetization from A to B (M_A . K_{for}) is equal to the transfer of magnetization from B to A (M_B . K_{rev}).

In more general terms, the rate of change of magnetization in the A pool, $dM_A(t)/dt$, is given by:

$$dM_A(t)/dt = (M_{A0} - M_A(t)) \cdot R_{1A} - M_A(t) \cdot K_{for} + M_B(t) \cdot K_{rev} \quad (1)$$

When the B pool is selectively saturated (and kept in complete saturation!) a new equilibrium is created where the A pool has less available longitudinal magnetization (labelled M_{Asat}) and also a shorter longitudinal relaxation time constant (labelled T_{1sat}), with:

$$M_{Asat} = M_{A0} / (1 + K_{for} \cdot T_{1A}) \quad (2)$$

and:

$$1/T_{1sat} = R_{1A} + K_{for} \quad (3)$$

Re-arranging (2) and (3) results in

$$K_{for} = (1/T_{1sat}) \cdot (1 - M_{Asat}/M_{A0}) \quad (4)$$

or:

$$M_{Asat}/M_{A0} = 1 - K_{for} \cdot T_{1sat} \quad (5)$$

Note that magnetization transfer is a dynamic process. After selective saturation of the B pool, the equilibrium longitudinal magnetization M_{A0} is reduced exponentially to M_{Asat} with a time constant T_{1sat}. Moreover, the analytical solutions above assume complete and indefinite saturation of the B pool. More details are well described by Hajnal et al.[32]. More complex and detailed MTC models are still being developed[15, 19, 20].

A more intuitive understanding of these effects is shown in Figure 8. The B pool is now empty (complete saturation has taken place since there is no water in bathtub B) and water flows from A to B. A new equilibrium water level is established when the inflow (via tube R_{1A}) and outflow (via tube K_{for}) are in balance. The amount of water which flowed from A to B cannot flow backwards, because the B pool is continuously emptied (kept in saturation). It is also easy to understand that a larger exchange rate K_{for} will result in an even lower value for M_{Asat} (mathematically described in Formula 2).

Figure 9 shows that a larger outflow tube (larger K_{for}) will result in a lower equilibrium water level. This effect is comparable to the situation where the exchange rate K_{for} is unchanged but the T_{1A} is larger.

The smaller inflow tube (R_{1A}) will result in a lower equilibrium water level (Fig. 10). This effect is also known from clinical practice - a higher field strength will result in a larger magnetization transfer effect[9].

Ceckler et al.[7] showed experimentally that the exchange rate K_{for} is field strength independent. The lower value of M_{Asat} is the result of the higher T_1 relaxation values with higher main magnetic fields (Fig. 10).

Saturating pre-pulses

There are basically two methods to selectively destroy the 'bound pool'[31-41].

The first method employs the differences in widths of the resonance lines (Fig. 11). Frequency selective RF pulses are transmitted at a frequency offset Δf with respect to the central ^1H Larmor frequency. Using these off-resonance pulses it is possible to substantially saturate the broad resonance of the 'bound pool' while hardly affecting the 'free pool'. Note that such a pulse will not only destroy the spins with the specific off-resonance frequency: due to spin diffusion all the macromolecule protons will be affected. The lower water peak is the result of the magnetization transfer process.

The second method employs the differences in T_2 between the pools. Binomial RF pulses with a resultant zero degree pulse angle ('jump and return') are transmitted on-resonance. The most often used pulse is a $90°_x$ $90°_{-x}$ $90°_{-x}$ $90°_x$ pulse, with a pulse length < 0.5 ms per element. During such a pulse-train, the magnitude of the 'free proton' magnetization is not changed, but its direction is changed according to the flip angle of each RF element.

Due to the long T_2 (much longer than the duration of the RF elements) the magnetization is returned to the z-axis at the end of the binomial pulse. Magnetization of 'bound protons' with a

11

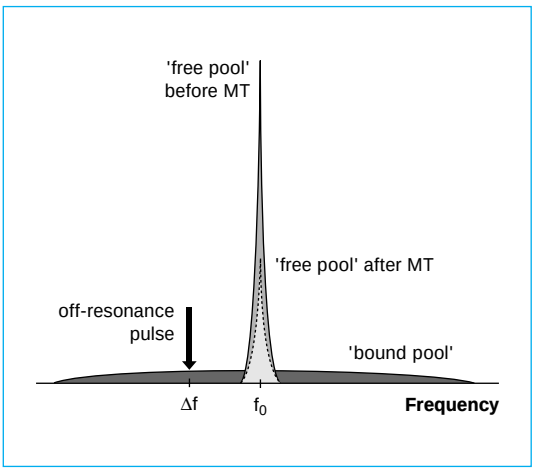

Fig. 11. Using off-resonance pulses it is possible to substantially saturate the broad resonance of the 'bound pool' while hardly affecting the 'free pool'. Due to spin diffusion all the macromolecule protons will be saturated. The lower water peak is the result of the magnetization transfer process.

Fig. 12. Simplified representation of the change of longitudinal magnetization M_z during a $90°_x$ $90°_{-x}$ pulse. Upper row represents the 'free pool', lower row represents the 'bound pool'. First column is the initial situation. The second column shows Mz and Mxy after a $90°_x$ excitation pulse. The third column shows the situation after some time Δt, with $\Delta t << T_2$ of the 'free pool' and $\Delta t >> T_2$ of the 'bound pool'. The fourth column shows M_z and M_{xy} after a $90°_{-x}$ reset pulse.

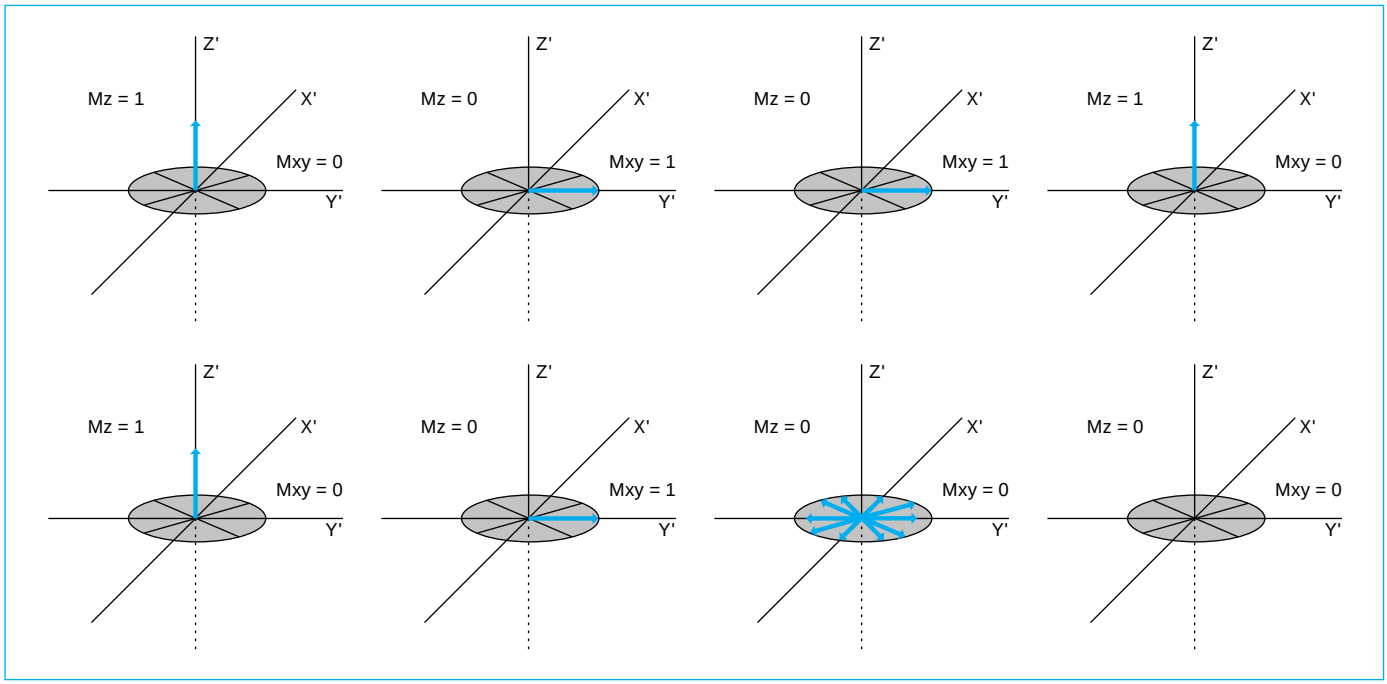

12

are destroyed (Figs 12, 13). Both methods should be considered as MTC pre-pulses which can be interleaved with all known MRI pulse sequences (Fig. 14). Depending on the clinical application, one can either use the induced changes in longitudinal magnetization (lower M_{Asat}) or the reduced longitudinal relaxation time constant (lower T_{1sat}) or a combination of both.

As a starting point for experimentation it is probably easiest to select a proton density weighted sequence and add either an on-resonance or an off-resonance MTC pre-pulse to generate the desired signal changes.

very short T_2 is destroyed, because the transverse dephasing is much faster than the duration of the RF elements. The net effect of such a pulse-train is that the magnetization of the 'free protons' is not changed and the 'bound protons'

13

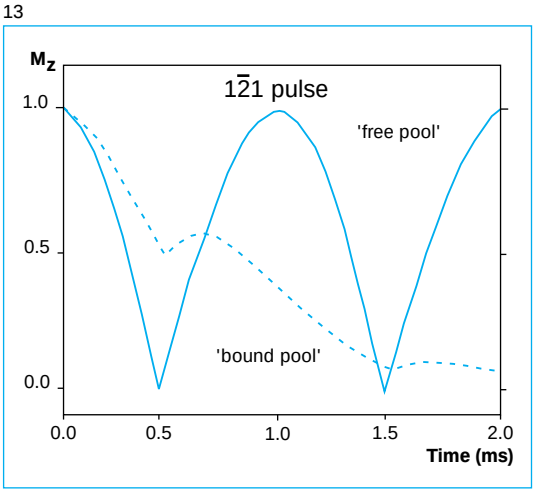

Fig. 13. The result of an on-resonance binomial pulse ($90°_x$ $90°_{-x}$ $90°_{-x}$ $90°_x$) for the 'free pool' is that the longitudinal magnetization M_z returns to its original value. The spins of the 'bound pool' with very short T_2 only experience decay, resulting in destroyed magnetization after the on-resonance pulse.

Because magnetization transfer is a dynamic process the MTC pre-pulses have to be repeated to keep the 'bound pool' saturated. As a rule of thumb, 10-20 MTC pre-pulses per second should be sufficient for complete saturation[37]. Depending on the software implementation on clinical scanners, the user can influence this by modifying repetition time TR and number of slices. On the Philips Gyroscan MR systems the MTC pre-pulses (either on-resonance or off-resonance), followed by a spoiler gradient to dephase any residual transversal magnetization, are applied before each excitation RF pulse (with Turbo Field Echo before each shot).

On-resonance and off-resonance pulses

The off-resonance pulse is a single, shaped RF pulse (e.g. sinc-Gauss) with a relatively narrow excitation bandwidth (dependent on pulse shape and duration). Two critical parameters will affect the amount of saturation: the

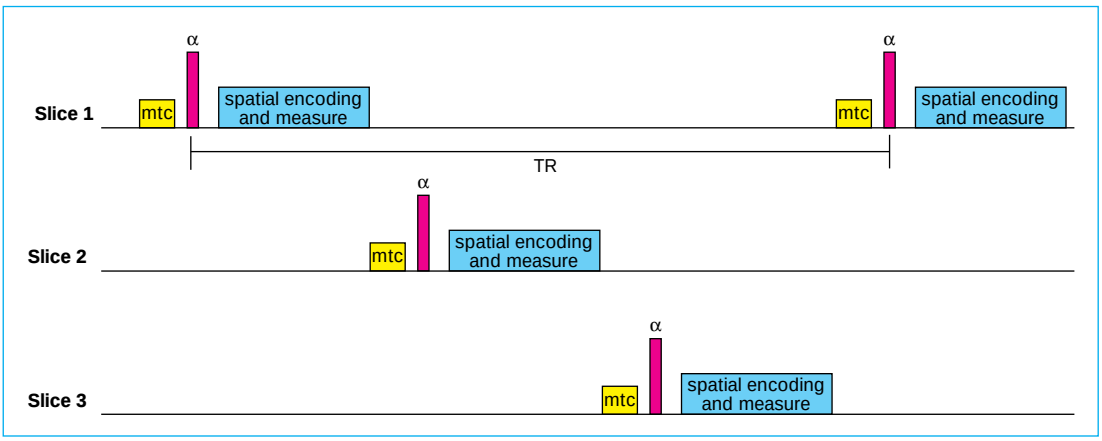

14

Fig. 14. MTC pre-pulses which can be interleaved with all known MRI pulse sequences. On the Philips Gyroscan systems the MTC pre-pulses (either on-resonance or off-resonance), followed by a spoiler gradient to dephase any residual transverse magnetization, are applied before each excitation RF pulse (α).

magnitude and the frequency offset of the off-resonance pulse[31-34, 38, 41].

More B_1 power will result in a better saturation, but is limited in practice by safety considerations (Specific Absorption Rate or SAR).

Decreasing the frequency offset will also create a better saturation of the 'bound pool', but values closer to the ^1H Larmor frequency will also result in direct excitation of the 'free pool'. A practical value is a 700° pulse angle of 10 ms applied at a frequency offset of 1500 Hz. For more details the user should refer to the operator's manual of the scanner used.

The on-resonance pulse is a composite RF pulse consisting of a series of rectangular (block) pulses. These binomial pulses can be considered as transparent for the 'free pool'. Several authors[35-37, 39-40] studied the optimal form ($1\bar{1}$, $1\bar{2}1$, $1\bar{3}3\bar{1}$ etc). From the Bloch equations one can show that higher order binomial pulses, with a shorter duration and a larger B_1, will result in a larger transparent bandwidth. This is the range of frequencies for which the 'free spins' are not affected after the pulse. Due to safety (SAR) and hardware limits a typical on-resonance pulse is a $1\bar{2}1$ pulse (4 elements) with a pulse angle of 90° and a duration per element of 0.3 ms.

In clinical practice, a practical problem at 1.5 T is the water-fat shift (WFS ≈ 220 Hz). The transparent bandwidth of the on-resonance MTC pre-pulse should be larger than the WFS, otherwise the fat spins will also be affected. Note that this has nothing to do with the actual magnetization transfer (cross relaxation), but is the direct result of the excitation bandwidth of the pulses used. Increasing the flip angle and decreasing the time duration of the on-resonance pulse elements will be helpful to increase the transparent bandwidth of the binomial pulse (Fig. 15). Again, the user should refer to the operator's manual of the scanner used.

The results of both methods for the magnetization transfer effects are basically similar, whereby the amount of saturation is a direct function of the B_1 power of the MTC pre-pulses. Theoretical simulations on the power efficiency[41] are probably bypassed by other factors in practical scanning, like SAR safety limits, desired contrast, and time efficiency.

Interleaving a standard MRI pulse sequence with MTC pre-pulses will increase TR with the time duration of the MTC pre-pulse and time for spoiling. This might be a disadvantage depending on the clinical application.

Incidental MTC

Dixon et al.[28] described the fact that MTC is implicitly generated in many normal imaging sequences where off-resonance pulses are applied. For example, in Spin Echo (SE) sequences the slice selective excitation and refocusing pulses can be considered as off-resonance pulse for neighbouring slices. This effect will also occur in 3D, spectral fat suppression and REST slabs (out-of-slice suppression).

In multislice TSE (Turbo SE, also called Fast SE) sequences this effect is significant due to the many 180° refocusing pulses[30]. Melki et al.[29] nicely demonstrated that the signal attenuation

15

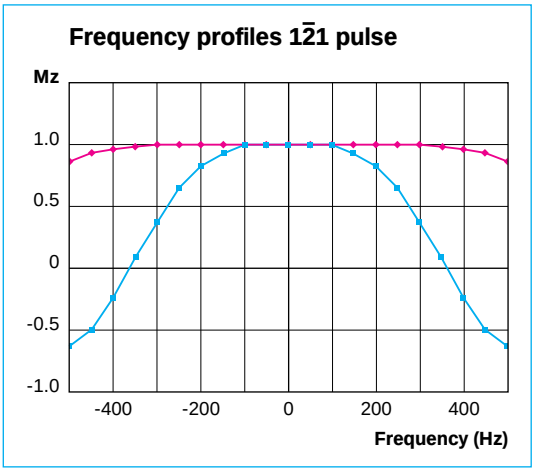

Fig. 15. The transparent bandwidth is the range of frequencies for which the 'free spins' are not affected after the pulse. Increasing the flip angle and decreasing the time duration of the on-resonance pulse increases the transparent bandwidth of the binomial pulse (squares). M_z is the longitudinal magnetization.

for white and grey brain matter in multislice sequences is a direct function of the number of slices. An example in knee joint imaging of the incidental MTC effect is shown in Figure 16.

Visualization of MTC

There are many ways to visualize the effects of the magnetization transfer process. The easiest way is to judge the MTC images directly. A more time-consuming way is to generate two sets of images, one with and one without MTC prepulses, and compare the changes in contrast qualitatively. A more quantitative approach is to construct synthetic images, for example a subtraction image or a ratio image. The first approach means that for each pixel the difference between two images is calculated and visualized; in the latter approach the relative change in signal intensity for each pixel is calculated. These subtraction or ratio images can be colour coded and overlaid on a high-resolution normal grey scale image. The most complex way is to calculate the actual rate of exchange of magnetization on a pixel basis. Theoretically, this is the most specific way of visualizing the MTC. Experimentally, it is more difficult because it requires measurement of several physical properties (M_{A0}, M_{Asat}, T_{1sat}, see Equation 4) and requires postprocessing of the data. The optimal solution of MTC visualization in routine scanning is dependent on the clinical application, scan time considerations and software for automatic generation of calculated images.

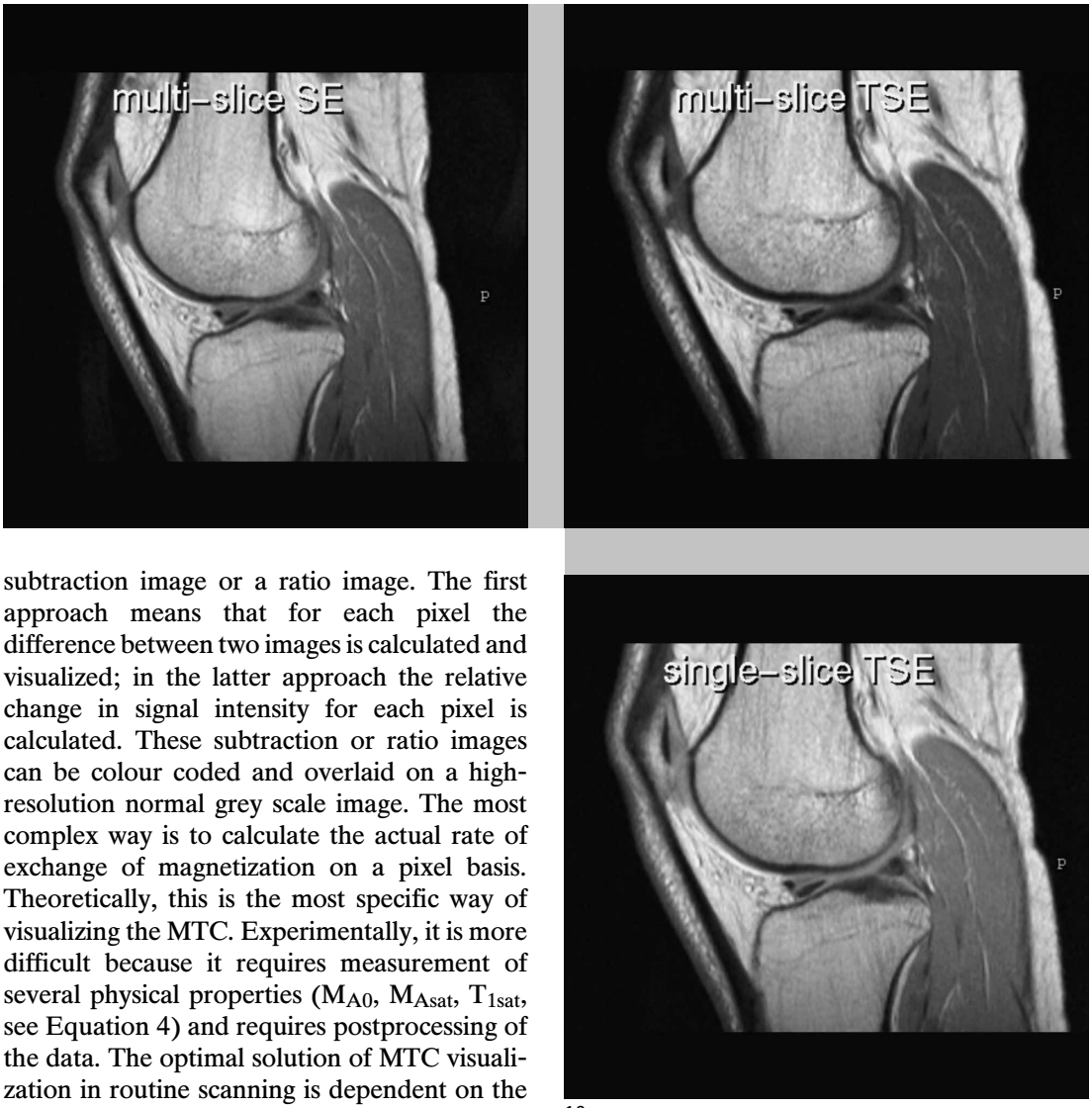

Fig. 16. MR images showing incidental MTC in knee joint imaging. Note the differences in cartilage and muscle intensity between multi-slice SE, multi-slice TSE and single-slice TSE.

Acknowledgements

The author gratefully acknowledges the contributions of M.K. Kouwenhoven MSc, L.H. Hofland MSc, S. Sheppard MSc, J.A. den Boer PhD, M.S. Silver PhD, A.R. Gillams MD, M. Vahlensieck MD, D.J. Jensen PhD, H.J. Kooijman PhD and M. Beese MD, in understanding the MR physics and applications of MTC.

References

Original publications

1. Forsén S, Hoffman RA. Study of Moderately Rapid Chemical Exchange Reactions by Means of Nuclear Magnetic Double Resonance. J Chem Phys 1963; 39: 2892-2901.
2. Edzes HT, Samulski ET. Cross Relaxation and Spin Diffusion in the Proton NMR of Hydrated Collagen. Nature 1977; 265: 521-523.
3. Edzes HT, Samulski ET. The Measurement of Cross-Relaxation Effects in the Proton NMR Spin-Lattice Relaxation of Water in Biological Systems: Hydrated Collagen and Muscle. J Magn Reson 1978; 31: 207-229.
4. Wolff SD, Balaban RS. Magnetization Transfer Contrast (MTC) and Tissue Water Proton Relaxation In Vivo. Magn Reson Med 1989; 10: 135-144.
5. Eng J, Ceckler TL, Balaban RS. Quantitative ^{1}H Magnetization Transfer Imaging In Vivo. Magn Reson Med 1991; 17: 304-314.

6. Wolff SD, Eng J, Balaban RS. Magnetization Transfer Contrast: Method for Improving Contrast in Gradient-Recalled-Echo Images. Radiology 1991; 179: 133-137.

Review papers
7. Balaban RS, Ceckler TL. Magnetization Transfer Contrast in Magnetic Resonance Imaging. Magn Reson Q 1992; 8(2): 116-137.
8. Bryant RG, Lester CC. Magnetic Relaxation Coupling in Heterogeneous Systems. J Magn Reson (series B) 1993; 101: 121-125.
9. Wolff SD, Balaban RS. Magnetization Transfer Imaging: Practical Aspects and Clinical Applications. Radiology 1994; 192: 593-599.
10. Santyr GE, Mulkern RV. Magnetization Transfer in MR Imaging. Magn Reson Imaging 1995; 5: 121-124.

Relaxation mechanisms
11. Morris GA, Freemont AF. Direct Observation of the Magnetization Exchange Dynamics Responsible for Magnetization Transfer Contrast in Human Cartilage In Vivo. Magn Reson Med 1992; 28: 97-104.
12. Brown III RD, Koenig SH. $1/T_1\rho$ and Low-Field $1/T_1$ of Tissue Water Protons Arise from Magnetization Transfer to Macromolecular Solid-State Broadened Lines. Magn Reson Med 1992; 28: 145-152.
13. Sepponen R. Rotating Frame and Magnetization Transfer. Chapter 8 in: Stark DS, Bradley WG (eds). Magnetic Resonance Imaging. 2nd ed. St. Louis, Mo: Mosby Year Book, 1992; 204-218.
14. Koenig SH, Brown RD, Ugolini R. Magnetization Transfer in Cross-Linked Bovine Serum Albumin Solutions at 200 MHz: a Model for Tissue. Magn Reson Med 1993; 29(3): 311-317.
15. Henkelman RM, Huang X, Xiang Q, Stanisz GJ, Swanson SD, Brosnkill MJ. Quantitative Interpretation of Magnetization Transfer. Magn Reson Med 1993; 29: 759-766.
16. Yeung HN. On the Treatment of the Transient Response of a Heterogeneous Spin System to Selective RF Saturation (letter to the editor). Magn Reson Med 1993; 30: 201-206.
17. Yang H, Schleich T. T_1 Discrimination Contributions to Proton Magnetization Transfer in Heterogeneous Biological Systems. Magn Reson Med 1994; 32(1): 16-22.
18. McGowan JC, Leigh JS jr. Selective Saturation in Magnetization Transfer Experiments. Magn Reson Med 1994; 32(4): 517-522.
19. Henkelman RM, Stanisz GJ, Kim JK, Bronskill MJ. Anisotropy of NMR Properties of Tissues. Magn Reson Med 1994; 32(5): 592-601.
20. Morrison C, Henkelman RM. A Model for Magnetization Transfer in Tissues. Magn Reson Med 1995; 33: 475-482.
21. Harrison R, Bronskill MJ, Henkelman RM. Magnetization Transfer and T_2 Relaxation Components in Tissue. Magn Reson Med 1995; 33: 490-496.

Dynamics of magnetization transfer
22. Rydzy M, Deslauriers R, Smith ICP, Saunders JK. Optimization of Magnetization Transfer Measurements: Statistical Analysis by Stochastic Simulation. Application to Creatine Kinase Kinetics. Magn Reson Med 1990; 15: 260-274.
23. Komu M. Analysis of Longitudinal Relaxation Rate Constants from Magnetization Transfer MR Images of Human Tissues at 0.1 T. Magn Reson Imaging 1992; 10: 35-40.
24. Mora BM, Narasimhan PT, Ross BD. ^{31}P Magnetization Transfer Studies in the Monkey Brain. Magn Reson Med 1992; 26: 100-115.
25. Boer RW de, Elevelt AJ. Turbo-MIX T_1 Measurements and MTC Exchange Rate K_{for} Calculations. Proceedings of The SMRM, 12th annual Meeting New York, 1993; 1: 175.
26. Schick F, Forster J, Pfeffer M, Lutz. O. Pulsed Magnetization Transfer for Imaging and Spectroscopic Applications on Whole-Body Imagers. MAGMA 1994; 2: 127-137.
27. Taitelbaum H, Weiss GH, Spencer RGS. Optimization of Magnetization Transfer Experiments for Kinetic Rate Measurements. NMR in Biomedicine 1994; 7: 287-292.

Incidental MTC
28. Dixon TW, Engels H, Castillo M, Shardashti M. Incidental Magnetization Transfer Contrast in Standard Multislice Imaging. Magn Reson Imaging 1990; 8: 417-422.
29. Melki PS, Mulkern RV. Magnetization Transfer Effects in Multislice RARE Sequences. Magn Reson Med 1992; 24: 189-195.
30. Santyr GE. Magnetization Transfer Effects in Multislice MR Imaging. Magn Reson Imaging 1993; 11(4): 521-532.

Pulse sequences
31. Ordidge RJ, Knight RA, Helpern JA. Magnetization Transfer Contrast (MTC) in Flash MR Imaging . Magn Reson Imaging 1991; 9: 889-893.
32. Hajnal JV, Baudouin CJ, Oatridge A, Young IR, Bydder GM. Design and Implementation of Magnetization Transfer Pulse Sequences for Clinical Use. J Comput Assist Tomogr 1992; 16(1): 7-18.
33. Dixon WT. Use of Magnetization Transfer Pulse Sequences for Clinical Use. J Comput Assist Tomogr 1992; 16: 7-18.
34. Swallow CE, Kahn CE jr, Halbach RE, Tanttu JI, Sepponen RE. Magnetization Transfer Contrast Imaging of the Human Leg at 0.1 T: a Preliminary Study. Magn Reson Imaging 1992; 10(3): 361-364.
35. Yeung HN, Aisen AM. Magnetization Transfer Contrast with Periodic Pulsed Saturation. Radiology 1992, 183: 209-214.
36. Hu BS, Conolly SM, Wright GA, Nishimura DG, Macovski A. Pulsed Saturation Transfer Contrast. Magn Reson Med 1992; 26: 231-240.
37. Schneider E, Prost RW, Glover GH. Pulsed Magnetization Transfer versus Continuous Wave Irradiation for Tissue Contrast Enhancement. Magn Reson Imaging 1993; 3: 417-423.
38. Jones RA, Southon TE. A Magnetization Transfer Preparation Scheme for Snapshot FLASH Imaging. Magn Reson Med 1993; 19: 483-488.
39. Pike GB, Glover GH, Hu BS, Enzmann DR. Pulsed Magnetization Transfer Spin-echo MR Imaging. Magn Reson Imaging 1993; 3: 531-539.
40. McGowan JC, Schnall MD, Leigh JS. Magnetization Transfer Imaging with Pulsed Off-Resonance Saturation: Variation in Contrast with Saturation Duty Cycle. Magn Reson Imaging 1994; 4: 79-82.
41. Hua J, Hurst GC. Analysis of On- and Off-Resonance Magnetization Transfer Techniques. Magn Reson Imaging 1995; 5: 113-120.